Biochemistry

 Volume 40, Number 34 August 28, 2001

Accelerated Publications

Subsite Specificity of Memapsin 2 (β-Secretase): Implications for Inhibitor Design[†]

Robert T. Turner III,[‡,§] Gerald Koelsch,[‡,||] Lin Hong,[‡,||] Pedro Castanheira,[‡,⊥] Arun Ghosh,[||,#] and Jordan Tang*[,‡,§,||]

Protein Studies Program, Oklahoma Medical Research Foundation, and Department of Biochemistry and Molecular Biology, University of Oklahoma Health Sciences Center, Oklahoma City, Oklahoma 73104, Zapaq, Inc., Oklahoma City, Oklahoma 73104, and Department of Chemistry, University of Illinois at Chicago, Chicago, Illinois 60607

Received May 30, 2001; Revised Manuscript Received June 29, 2001

ABSTRACT: Memapsin 2 is the protease known as β-secretase whose action on β-amyloid precursor protein leads to the production of the β-amyloid (Aβ) peptide. Since the accumulation of Aβ in the brain is a key event in the pathogenesis of Alzheimer's disease, memapsin 2 is an important target for the design of inhibitory drugs. Here we describe the residue preference for the subsites of memapsin 2. The relative k_{cat}/K_M values of residues in each of the eight subsites were determined by the relative initial cleavage rates of substrate mixtures as quantified by MALDI-TOF mass spectrometry. We found that each subsite can accommodate multiple residues. The S_1 subsite is the most stringent, preferring residues in the order of Leu > Phe > Met > Tyr. The preferences of other subsites are the following: S_2, Asp > Asn > Met; S_3, Ile > Val > Leu; S_4, Glu > Gln > Asp; S_1', Met > Glu > Gln > Ala; S_2', Val > Ile > Ala; S_3', Leu > Trp > Ala; S_4', Asp > Glu > Trp. In general, S subsites are more specific than the S′ subsites. A peptide comprising the eight most favored residues (Glu-Ile-Asp-Leu-Met-Val-Leu-Asp) was found to be hydrolyzed with the highest k_{cat}/K_M value so far observed for memapsin 2. Residue preferences at four subsites were also studied by binding of memapsin 2 to a combinatorial inhibitor library. From 10 tight binding inhibitors, the consensus preferences were as follows: S_2, Asp and Glu; S_3, Leu and Ile; S_2', Val; and S_3', Glu and Gln. An inhibitor, OM00-3, Glu-Leu-Asp-Leu*Ala-Val-Glu-Phe (where the asterisk represents the hydroxyethylene tansition-state isostere), designed from the consensus residues, was found to be the most potent inhibitor of memapsin 2 so far reported (K_i of 3.1×10^{-10} M). A molecular model of OM00-3 binding to memapsin 2 revealed critical improvement of the interactions between inhibitor side chains with enzyme over a previous inhibitor, OM99-2 [Ghosh, A. K., et al. (2000) *J. Am. Chem. Soc. 14*, 3522−3523].

The accumulation of β-amyloid peptide (Aβ)[1] in the brain is a major factor underlying the pathogenesis of Alzheimer's disease (AD) (*1*). Aβ is a fragment of a brain membrane protein β-amyloid precursor protein (APP) produced by the activity of two proteases known as β- and γ-secretases. β-Secretase cleaves APP first in its lumenal domain and

[†] This work was partly supported by NIH Grant AG-18933. R.T.T. is a recipient of a Glenn/American Foundation for Aging Research Scholarship. G.K. is a Scientist Development Grant Awardee of the American Heart Association. J.T. is holder of the J. G. Puterbaugh Chair in Biomedical Research at the Oklahoma Medical Research Foundation.

* To whom correspondence should be addressed at the Oklahoma Medical Research Foundation, 825 NE 13 St., Oklahoma City, OK 73104. Email: jordan-tang@omrf.ouhsc.edu. Tel: 405-271-7291. FAX: 405-271-7249.

[‡] Oklahoma Medical Research Foundation.

[§] University of Oklahoma Health Sciences Center.

[||] Zapaq, Inc.

[⊥] Present address: Department of Biochemistry, University of Coimbra, Coimbra, Portugal.

[#] University of Illinois at Chicago.

[1] Abbreviations: Aβ, β-amyloid peptide; APP, β-amyloid precursor protein; AD, Alzheimer's disease.

10.1021/bi015546s CCC: $20.00
Published on Web 08/03/2001

commits the C-terminal fragment of APP to hydrolysis by γ-secretase, thus generating Aβ (for review, see refs *1* and *2*). Since β-secretase catalyzes the first step in Aβ production and its activity is common for the pathogenesis of all forms of familial and sporadic AD, this protease is considered to be an important target of inhibitory drugs for the treatment of the disease.

Recently, our group (*3*) and others (*4*−*7*) independently cloned a human brain aspartic protease, which we named memapsin 2 (*3*). Other names given were BACE (*4*), ASP-2 (*5*, *7*), and 'β-site APP-cleaving enzyme' (*6*). We demonstrated that memapsin 2 fits all the known criteria of the β-secretase (*3*), a conclusion also reached by these other groups. Memapsin 2 cDNA encodes for pre, pro, protease, transmembrane, and intracellular regions. The zymogen domain of pro-memapsin 2 is an independent folding unit and is proteolytically active (*3*) because its pro-peptide only covers the active site part of the time (*8*). In contrast to pepsinogen-like zymogens, pro-memapsin 2 does not spontaneously convert to memapsin 2 in acid solutions. Digestion of recombinant pro-memapsin 2 by proteases such as clostripain resulted in the removal of segments of the pro-peptide and the increase of enzymic activity (*8*). Limited specificity information, generated from the hydrolysis of several peptides (*3*), was used to design an inhibitor, OM99-2, an eight residue transition-state analogue (*9*). A 1.9 Å crystal structure of the memapsin 2 protease domain complexed to OM99-2 (*10*) clearly defined the location and topology of the eight subsites in the substrate binding cleft of the enzyme. These results demonstrate that by evoking all eight subsites with OM99-2, a high inhibition potency (K_i = 1.6 nM, ref *8*) can be achieved. However, clinically useful memapsin 2 inhibitors must be small in size (i.e., <500 daltons) to penetrate the blood−brain barrier. Detailed information on the subsite specificity of memapsin 2 would render a better understanding for the design of small yet tight-binding inhibitors. We report here the complete subsite preference of memapsin 2 based on results from both substrate kinetics and the screening of a combinatorial inhibitor library.

EXPERIMENTAL PROCEDURES

Design of the Defined Substrate Mixtures. The peptide sequence EVNLAAEF, known to be a memapsin 2 substrate and inhibitor (*9*), was used as a template structure to study residue preferences in substrate mixtures. For characterization of each of the eight subsites, separate substrate mixtures were obtained by addition of an equimolar mixture of six or seven amino acid derivatives in the appropriate cycle of solid-phase peptide synthesis (Research Genetics, Invitrogen, Huntsville, AL). The resulting mixture of six or seven peptides differed only by one amino acid at a single subsite. We had previously established that limiting the number of peptides in a mixture facilitated their identification (*11*). Thus, at each subsite, 19 varied amino acids (less cysteine) were accommodated in 3 substrate mixtures, requiring 24 substrate mixtures to characterize 8 subsites. A substrate of known k_{cat}/K_M was also added to each mixture to serve as an internal standard. To facilitate the analysis in MALDI-TOF MS, the template sequence was extended by four residues at the C-terminus (EVNLAAEFWHDR) for variations at P_1', P_2', P_3', and P_4' and at the N-terminus (RWHHEVNLAAEF) to study positions P_1, P_2, P_3, and P_4.

Initial Rate Determination by MALDI-TOF Mass Spectrometry. Substrate mixtures were dissolved at 2 mg/mL in 10% glacial acetic acid and diluted into 0.009 M NaOH to obtain a mixture of substrates in the micromolar range at pH 4.1. After equilibration at 25 °C, the reactions were initiated by the addition of an aliquot of Leu^{28P}-memapsin 2 (*8*). Aliquots were removed at time intervals, and combined with an equal volume of MALDI-TOF matrix (α-hydroxycinnamic acid in acetone, 20 mg/mL) and immediately spotted in duplicate onto a stainless-steel MALDI sample plate. MALDI-TOF mass spectrometry was performed on a PE Biosystems Voyager DE instrument at the Molecular Biology Resource Center on campus. The instrument was operated at 25 000 accelerating V in the positive mode with a 150 ns delay. Ions with a mass-to-charge ratio (*m*/z) were detected in the range of 650−2000 atomic mass units. Data were analyzed by the Voyager Data Explorer module to obtain ion intensity data for mass species of substrates and corresponding products in a given mixture. Relative product formation was calculated as the ratio of signal intensity of the product to the sum of signal intensities of both product and the corresponding substrate. The quantitative aspect of this analysis was established as follows. From a mixture consisting of seven substrate peptides, EVNL**X**AEFWHDR (**X** = amino acids A, S, T, I, D, E, and F), their hydrolytic peptide products, **X**AEFWHDR, were prepared by complete proteolysis. A series of mock partial digestions was prepared by combining known amounts of the substrate mixture with the hydrolysate, and each was subjected to MALDI-TOF/MS analysis. The ratios of product to sum of product and substrate peptide from observed intensity data correlated with the expected ratios for each pair of peptides in the mixture (average slope 0.94 ± 0.06; average correlation coefficient 0.92 ± 0.04). Relative product formed per unit time was obtained from nonlinear regression analysis of the data representing the initial 15% formation of product using the model:

$$1 - e^{-kT}$$

where k is the relative hydrolytic rate constant and T is the time in seconds. The initial relative hydrolytic rates of unknown substrates were converted to the relative k_{cat}/K_M by the equation:

$$\text{relative } k_{cat}/K_M = v_x/v_s$$

where v_x and v_s are the initial hydrolytic rates of substrate x and the reference substrates (*12*−*14*). For convenience of discussion, the relative k_{cat}/K_m value is also referred to as "preference index".

Random Sequence Inhibitor Library. The combinatorial inhibitor library was based on the sequence of OM99-2, EVNL*AAEF (*9*) (where the asterisk represents the hydroxyethylene transition-state isostere), with random amino acids (less cysteine) at four subsites: P_2, P_3, P_2', and P_3'. The di-isostere Leu*Ala was used in a single step of the synthesis (*9*), thus fixing the structures at positions P_1 and P_1'. Peptides were synthesized by the solid-phase peptide synthesis method and left attached on the resin beads. By using the 'split-synthesis' procedure (*15*), each of the resin

beads contained only one sequence while the sequence differed from bead to bead. The overall library sequence was

Gly-Xx1-Xx2-Leu*Ala-Xx3-Xx4-Phe-Arg-Met-Gly-Gly-[Resin bead]

P_4 P_3 P_2 P_1 P_1' P_2' P_3' P_4'

where Xx*n* residues (where *n* represents either 1, 2, 3, or 4) are randomized at each position with 19 amino acids. A shorter version of the peptides, starting at P_2' (sequence: Xx3-Xx4-Phe-Arg-Met-Gly-Gly-[resin bead]), was also present in each bead with a ratio to the longer sequence of about 7:3. Without the isostere, the short sequence would not bind memapsin 2 with significant strength, but its presence was convenient for identifying the residues at P_2' and P_3' by automated Edman degradation. The residues were identified from the randomized positions as follows:

Edman cycle # :	1	2	3	4
Sequence 1, from the long sequence:	Gly	Xx1	Xx2	
Sequence 2, from the short sequence:	Xx3	Xx4	Phe	Arg

The assignments of Xx3 and Xx2 had no ambiguity since they are the only unknown residues at cycles 1 and 3, respectively. Amino acids Xx1 and Xx4 were assigned from their relative amounts. The presence of a methionine was designed to permit MS/MS identification of peptide fragments from those released following CNBr cleavage. This, however, proved unnecessary.

Probing of the Random Sequence Library. About 130 000 individual beads, representing 1 copy of the library and estimated to be contained in 1.1 mL of settled beads, were hydrated in buffer A (50 mM sodium acetate, 0.1% Triton X-100, 0.4 M urea, 0.02% sodium azide, 1 mg/mL bovine serum albumin, pH 3.5; filtered with a 5 μm filter). The beads were soaked in 3% bovine serum albumin in buffer A for 1 h, to block nonspecific binding, and rinsed twice with the same buffer. Recombinant memapsin 2 was diluted into buffer A to 4 nM and incubated with the library for 1 h. A single stringency wash was performed which included 6.7 μM transition-state isosteric inhibitor OM99-2 (*9*) in buffer B (50 mM sodium acetate, 0.1% Triton X-100, 0.02% sodium azide, 1 mg/mL BSA, pH 5.5; filtered with a 5 μm filter), followed by two additional washes with buffer B without OM99-2. Affinity-purified IgG specific for recombinant memapsin 2 (*3*) was diluted 100-fold in buffer B and incubated 30 min with the library. Following three washes with buffer B, affinity-purified anti-goat/alkaline phosphatase conjugate was diluted into buffer B (1:200) and incubated for 30 min, with three subsequent washes. A single tablet of alkaline phosphatase substrate (BCIP/NBT; Sigma) was dissolved in 10 mL of water, of which 1 mL was added to the beads and incubated 1 h. Beads were resuspended in 0.02% sodium azide in water and examined under a dissecting microscope. Darkly stained beads were graded by sight, individually isolated, stripped in 8 M urea for 24 h, and destained in dimethylformamide. The sequence determination of the beads was carried out using an Applied Biosystem Protein Sequencer at the Molecular Biology Resource Center on campus. The phenylthiohydantoin-amino acids were quantified using reversed-phase high-pressure liquid chromatography.

Synthesis of Inhibitor OM00-3. This inhibitor (E**LD**L*A**VE**F) was synthesized using the method as described by Ghosh et al. (*9*).

Determination of Kinetic Parameters. The kinetic parameters, K_M and k_{cat}, using single peptide substrate, and K_i against free inhibitors, were determined as previously described (*8*).

Model Building of OM00-3 Binding to Memapsin 2. The crystal structure of OM99-2 in complex with memapsin 2 was used as the initial model. Corresponding subsite residues were replaced with that of the OM00-3. The side chain conformations were visually selected from a rotomer library for the best fitting into the binding pockets in terms of the nonbonded interactions. Energy minimization was then carried out with the CNS program using Engh and Huber energy parameters (*16*). Cα atoms and the atoms with a distance of more than 5 Å from the inhibitor were subjected to harmonic restraint during the minimization process.

RESULTS AND DISCUSSION

Determination of Substrate Side-Chain Preference in Memapsin 2 Subsites. The substrate cleft of memapsin 2 accommodates eight side chains as shown in the crystal structure (*10*). To analyze a complete set of side chain preference by classical enzyme kinetics for all subsites of memapsin 2 would require the determination of 160 pairs of individual k_{cat} and K_M values, a tedious task so far not attained for any aspartic protease with broad specificity. The residue preferences at each subsite for different substrate side chains are defined by the relative k_{cat}/K_M values, which are, however, directly related to the relative initial hydrolysis rates of these mixtures of competing substrates under the condition that the substrate concentration is lower than K_M (*12*). This provides a less laborious method to determine the residue preference by measuring the initial velocity of substrate mixtures. This method has been successfully used to analyze the specificity of other aspartic proteases (*11*, *13*). We further simplified the rate determination by the use of MALDI-TOF/MS ion intensities for quantitation of relative amounts of products and substrates.

The substrate side chain preferences, reported as 'preference index' in eight subsites of memapsin 2, are presented in Figure 1. These results confirm our previous observation (*3*) that none of the eight subsites of memapsin 2 is absolutely stringent for substrate side chains. On both the P side and the P′ side, the subsites proximal to the scissile bond (P_1 and P_1') are more stringent than the distal subsites (P_4 and P_4'). This is evident when the preference indexes of the nonpreferred residues (background levels) are compared to the preferred residues. The lack of stringency is more pronounced for the four subsites on the P′ side, especially for P_3' and P_4' where the background is relatively high. The poor stringency of these two subsites is consistent with the observation that the P_3' and P_4' side chains of OM99-2 do not significantly interact with the enzyme in the crystal structure (*10*).

Subsite P_4 favors residues in the order of Glu, Gln, and Asp. P_4-Glu of OM99-2 fits well in the S_4 pocket with multiple interactions (*10*). The reduction of catalytic efficiency from substitution of P_4-Glu with Gln may be due to the loss of charge interaction of the P_4 side chain with

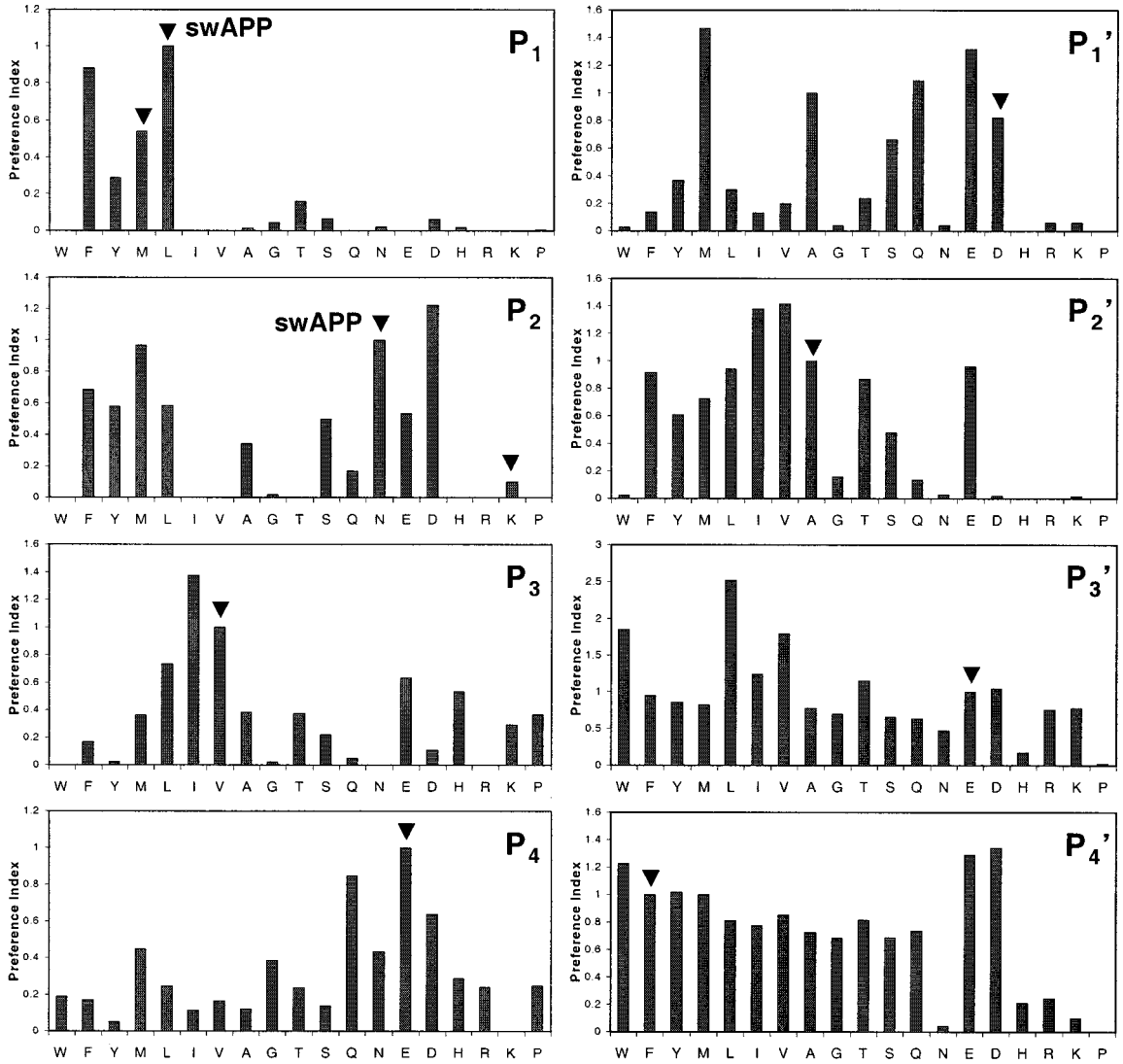

FIGURE 1: Preference of amino acid residues in the eight subsites of memapsin 2 substrates. The preference index (see Experimental Procedures) was calculated from the relative initial hydrolytic rates of mixed substrates and is proportional to the relative k_{cat}/K_M (*12*−*14*). Amino acids (single-letter code) appear in the substrate template sequence at the position designated in each panel (P_n or P_n'). The arrows indicate the residues found in native APP or Swedish mutant APP (labeled swAPP).

Arg^{235} and Arg^{307}. The further decrease of catalytic efficiency from substitution of P_4-Glu with Asp is likely due to the loss of the hydrogen bond to P_2-Asn (*10*). For subsite P_3, an Ile is more preferable than the Val in OM99-2. This is due to a better fit in the S_3 hydrophobic pocket as will be shown in the model below. The preference of the P_2 residue is clearly Asp or Asn. Memapsin 2 S_2 is relatively hydrophilic, and the ability of the P_2 side chain to form a hydrogen bond to P_4 may also be important for catalytic efficiency (*10*). Although P_1 is by far the most stringent subsite, three side chains (Leu, Phe, and Met) can still be accommodated. All four P′ subsites are very nonspecific, as the preference indexes of the best residues are not far from lesser ones. We have shown that in the familial AD caused by the Swedish mutation of APP, the change of P_2-P_1 from Lys-Met to Asn-Leu results in an increase of about 60-fold of the k_{cat}/K_M of memapsin 2 cleavage (*3*). The current results suggest that the greatest increase in catalytic efficiency is derived from the change in P_2 (Figure 1). An Asp or Met at this position accompanied by a P_1-Leu may also elevate the Aβ production and cause AD. However, both of these changes require two or more nucleotide replacements and are therefore less frequent genetic events. It is interesting to note that the P′ residues of APP are not among the most preferred by memapsin 2 (Figure 1); but due to the lack of stringency of these subsites, their catalytic efficiencies are not far from those for the best residues.

Side-Chain Preference Determined from a Combinatorial Inhibitor Library. As an alternative approach, the preference of memapsin 2 binding to side chains was also studied using a combinatorial library. The base sequence of the library was taken from OM99-2: E**VN**L*A**AE**F (the asterisk designates the isostere hydroxyethylene) (*9*), in which the subsites P_3, P_2, P_2', and P_3' (boldface) were randomized with all amino acids except cysteine. After incubating the bead library with memapsin 2 and stringent selection of washing with OM99-2 solution, about 65 beads from nearly 130 000 beads were darkly stained, indicating strong memapsin 2 binding. The residues at the 4 randomized positions were determined for the 10 most intensely stained beads. Table 1 shows that there is a clear consensus at these positions. This consensus is not present in the sequence of two negative controls (Table 1). These observations support the conclusion that washing the memapsin 2-bound beads with a strong inhibitor, OM99-2

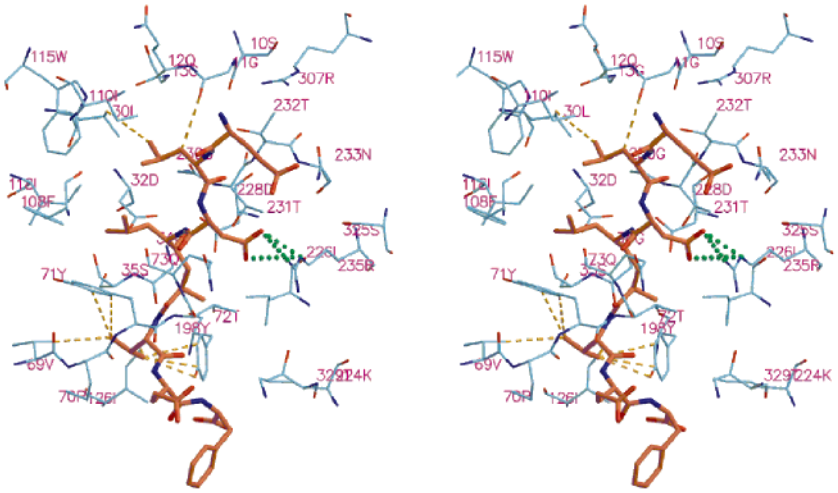

FIGURE 2: Stereo presentation of OM00-3 binding to memapsin 2. The yellow dotted lines represent the additional hydrophobic and van der Waal interactions between the inhibitor and the new binding pocket residues compared to the OM99-2 complex. The green dotted lines indicate the additional salt bridge interactions introduced by changes in the P_2 subsite. Residues of memapsin 2 which comprise the binding subsites are shown.

Table 1: Observed Residues at 4 Subsites from 10 Beads with Bound Memapsin 2 Selected from a Combinatorial Inhibitor Library[a]

ID	P_3	P_2	P_2'	P_3'
1	Leu	Asp	Val	Glu
2	Leu	Glu	Val	Glu
3	Leu	Asp	Val	Glu
4	Leu	Asp	Val	Glu
5	Leu	Asp	Val	Gln
6	Ile	Asp	Ala	Gln
7	Ile	Asp	Val	Tyr
8	Leu	Glu	Val	Gln
9	Leu	Phe	Val	Glu
10	Phe/Ile	Ser	Val	Phe/Ile
Neg1[b]	Phe	Met	Asn	Arg
Neg2[b]	Asp	Phe		Ser

[a] Library template: Gly-P_3-P_2-Leu*Ala-P_2'-P_3'-Phe-Arg-Met-Gly-Gly-resin. [b] Neg1 and Neg2 are two randomly selected beads with no memapsin 2 binding capacity.

(K_i = 1.6 nM), was an effective stringency selection for preferred binding sequences of inhibitors. A new inhibitor, OM00-3, E**LD**L*A**VE**F, was designed based on the consensus and synthesized. OM00-3 was found to inhibit memapsin 2 with a K_i of 0.31 nM, nearly 5-fold lower than the K_i of OM99-2 (*8*). In addition, the residue preferences determined at P_3, P_2, and P_2' of the inhibitors agreed well with the results from substrate studies (Figure 1). However, the preferred residues from P_3' observed from the inhibitor library were Glu or Gln, which ranked seventh in substrate residue preference at this position (Figure 1). The discrepancy may have stemmed from the lack of an effective S_3' subsite in memapsin 2 (*10*). It may also reflect the subtle differences in the steric requirement for binding substrate at the transition state as opposed to binding of transition-state mimics.

Catalytic Efficiency of Substrate Designed from Consensus Preference Residues. Based on the observed residue preferences, we also designed a new substrate and studied its hydrolytic efficiency by memapsin 2. Peptide *OK*, **EIDLMVLD**WHDR, was designed from the most preferred residues (boldface) identified from substrate studies (Figure 1) with the residues WHDR added to facilitate detection in MALDI-TOF/MS. Peptide *SW*, **EVNLDAEF**WHDR, was derived from the APP β-secretase site with Swedish mutation. The kinetic parameters for memapsin 2 hydrolysis of the peptide substrates (Table 2) indicate that the optimized substrate, *OK*, was cleaved with a k_{cat}/K_M value about 14-fold better than that of peptide *SW*. Interestingly, the enhancement is due to improvement in the K_M, whereas k_{cat} changed much less. We have shown that peptide derived from the β-secretase site of Swedish APP has a k_{cat}/K_M value about 60-fold higher than that from native APP (*3*). Therefore, the catalytic efficiency for the optimized substrate *OK* should be several hundredfold higher than the native APP peptide. These observations suggest that physiological substrates of memapsin 2 with kinetic parameters approaching those of peptide *OK* would be much better substrates than native APP. Such a comparison is also consistent with the idea that memapsin 2 hydrolysis of native APP is a physiological aberration. The k_{cat} and k_{cat}/K_M values for peptide *SW* are 60-fold and 9.5-fold higher, respectively, than those for the fluorogenic substrate FS-2 (*8*) containing the same Swedish APP sequence. Since FS-2 contains two bulky fluorophore and quenching groups, we speculate that it may have some conformational hindrance to memapsin 2 hydrolysis.

Table 2: Kinetic Parameters for Memapsin 2-Catalyzed Cleavage of Substrates

peptide[a]	sequence	k_{cat} (min^{-1})	K_M (μM)	k_{cat}/K_M (min^{-1} μM^{-1})
OK	EIDLMVLDWHDR	28.6 ± 3	1.4 ± 0.2	20.8 ± 2
SW	EVNLDAEFWHDR	54.7 ± 11	35.8 ± 2	1.53 ± 0.3

[a] Consensus peptide substrate *OK* was derived from specificity determinations and peptide *SW* was derived from the β-secretase site of Swedish mutant of APP.

Implications on Inhibitor Binding to Memapsin 2 Subsites. Since the potency of inhibitor OM00-3 (K_i = 0.3 nM) is significantly improved from that of OM99-2 (K_i = 1.6 nM), the binding of OM00-3 to memapsin 2 was modeled and compared to the crystal structure of the OM99-2/memapsin 2 complex. The P_4, P_1, P_1', P_3', and P_4' side chains are the same in the two inhibitors. The interaction of the model inhibitor side chains with the other subsites, however,

provides some insight to the improved binding of OM00-3. The larger hydrophobic side chains at P_3 and P_2' subsites for OM00-3 are better accommodated by the enzyme subsite through improved van der Waal interactions. Among these are six significant new interactions: P_3-Leu of inhibitor with Leu^{30} and Gly^{11} of the enzyme and P_2'-Val with Val^{69}, Tyr^{71}, Ile^{126}, and Tyr^{198} (Figure 2). In addition, the model shows that replacement of Asn by Asp at the P_2 position introduces a new salt bridge with multiple interactions between the side-chain atoms OD1 and OD2 of P_2-Asp and NE and NH1 of Arg^{235} (Figure 2). These charge interactions with an average interatomic distance of 3.5 Å should render an improved free energy of binding over that of P_2-Asn in OM99-2. These observed structural differences between the binding of the two inhibitors are consistent with the 4.5-fold decrease in K_i values from OM99-2 (*8*) to OM00-3.

The current results demonstrate that complete subsite specificity information of an aspartic protease can be used to design better substrates and inhibitors. With a K_i of 0.3 nM, the inhibition potency of OM00-3 is near that of inhibitor drugs of human immunodeficiency virus protease. However, to be useful for clinical treatment of AD, memapsin 2 inhibitors must penetrate the blood−brain barrier, and, consequently, must be smaller than 500 Da for passive penetration of the barrier. The eight-residue inhibitor OM00-3, albeit potent, is 917 Da. For facilitated penetration, however, the blood−brain barrier permits the penetration of larger compounds, including the HIV protease inhibitor drug Indinavir (614 Da, ref *17*). A possible strategy for the design of clinically useful memapsin 2 inhibitors is to use fewer subsite interactions, perhaps spanning only four or five subsites of memapsin 2. The broad specificity of all subsites of memapsin 2 reported here implies that, as in the inhibitor design for HIV protease, numerous structures can be accommodated by each subsite, a favorable setting for finding kinetically and pharmaceutically acceptable inhibitors. Information described herein together with the information on the three-dimensional structure of the subsites (*10*) would facilitate the design of smaller yet potent memapsin 2 inhibitors.

ACKNOWLEDGMENT

We thank Dr. Ken Jackson of the Warren Medical Research Foundation, University of Oklahoma Health Sciences Center, for helpful suggestions in the design of the random peptide library.

REFERENCES

1. Selkoe, D. J. (1999) *Nature 399A*, 23−31.
2. Sinha, S., and Lieberburg, I. (1999) *Proc. Natl. Acad. Sci. U.S.A. 96*, 11049−11053.
3. Lin, X., Koelsch, G., Wu, S., Downs, D., Dashti, A., and Tang, J. (2000) *Proc. Natl. Acad. Sci. U.S.A. 97*, 1456−1460.
4. Vassar, R., Bennett, B. D., Babu-Khan, S., Kahn, S., Mendiaz, E. A., Denis, P., Teplow, D. B., Ross, S., Amarante, P., Loeloff, R., Luo, Y., Fisher, S., Fuller, J., Edenson, S., Lile, J., Jarosinski, M. A., Biere, A. L., Curran, E., Burgess, T., Louis, J. C., Collins, F., Treanor, J., Rogers, G., and Citron, M. (1999) *Science 286*, 735−741.
5. Yan, R., Bienkowski, M. J., Shuck, M. E., Miao, H., Tory, M. C., Pauley, A. M., Brashier, J. R., Stratman, N. C., Mathews, W. R., Buhl, A. E., Carter, D. B., Tomasselli, A. G., Parodi, L. A., Heinrikson, R. L., and Gurney, M. E. (1999) *Nature 402*, 533−537.
6. Sinha, S., Anderson, J. P., Barbour, R., Basi, G. S., Caccavello, R., Davis, D., Doan, M., Dovey, H. F., Frigon, N., Hong, J., Jacobson-Croak, K., Jewett, N., Keim, P., Knops, J., Kieberburg, I., Power, M., Tan, H., Tatsuno, G., Tung, J., Schenk, D., Seubert, P., Suomensaari, S. M., Wang, S., Walker, D., John, V., et al. (1999) *Nature 402*, 537−540.
7. Hussain, I., Powell, D., Howlett, D. R., Tew, D. G., Meek, T. D., Chapman, C., Gloger, I. S., Murphy, K. E., Southan, C. D., Ryan, D. M., Smith, T. S., Simmons, D. L., Walsh, F. S., Dingwall, C., and Christie, G. (1999) *Mol. Cell. Neurosci. 14*, 419−427.
8. Ermolieff, J., Loy, J. A., Koelsch, G., and Tang, J. (2000) *Biochemistry 39*, 12450−12456.
9. Ghosh, A. K., Shin, D., Downs, D., Koelsch, G., Lin, X., Ermolieff, J., and Tang, J. (2000) *J. Am. Chem. Soc. 14*, 3522−3523.
10. Hong, L., Koelsch, G., Lin, X., Wu, S., Terzyan, S., Ghosh, A. K., Zhang, X. C., and Tang, J. (2000) *Science 290*, 150−153.
11. Koelsch, G., Tang, J., Loy, J. A., Monod, M., Jackson, K., Foundling, S. I., and Lin, X. (2000) *Biochim. Biophys. Acta 1480*, 117−131.
12. Fersht, A. (1985) *Enzyme Structure and Mechanism*, 2nd ed., W. H. Freeman, New York.
13. Kassel, D. B., Green, M. D., Wehbie, R. S., Swanstrom, R., and Berman, J. (1995) *Anal. Biochem. 228*, 259−266.
14. Petithory, J. R., Masiarz, F. R., Kirsch, J. F., Santi, D. V., and Malcolm, B. A. (1991) *Proc. Natl. Acad. Sci. U.S.A. 88*, 11510−11514.
15. Lam, K. S., Salmon, S. E., Hersh, E. M., Hruby, V. J., Karmierski, W. M., and Knapp, R. J. (1991) *Nature 354*, 82−84.
16. Engh, R. A., and Huber, R. (1991) *Acta Crystallogr. A47*, 392−400.
17. Martin, C., Sonnerborg, A., Svennson, J. O., and Stahle, L. (1999) *AIDS 13*, 1227−1132.

BI015546S